urn:nbn:de:gbv:ilm1-2011imeko-015:6

Joint International IMEKO TC1+ TC7+ TC13 Symposium
August 31st – September 2nd, 2011, Jena, Germany
urn:nbn:de:gbv:ilm1-2011imeko:2

Characteristics of a Monolithically Integrated Micro-Displacement Sensor

Toshihiro Takeshita[1], *Yao Peng*[1], *Nobutomo Morita*[1], *Hideyuki Ando*[2], *Eiji Higurashi*[3] *and Renshi Sawada*[4]

[1] Graduate School of Systems Life Sciences Kyushu University, 744, Motooka, Nishi-ku, Fukuoka, Japan
[2] Fuzzy Logic Systems Institute, Kawazu, Iizuka, Fukuoka, Japan,
[3] Research Center for Advanced Science and Technology Tokyo University, Komaba, Meguro, Tokyo, Japan,
[4]Department of Intelligent Machinery and Systems, Kyushu University, 744, Motooka, Nishi-ku, Fukuoka-city, Japan

Abstract – The authors report on the development of an optical ultra-micro-displacement sensor with a simple structure that is 3.0 x 3.0 mm square and 1.3 mm thick, and fabricated using MEMS technology. The displacement sensor only consists of a vertical cavity surface emitting laser (VCSEL), eight two-dimensional monolithically integrated photodiodes (PDs), a frame and a cover glass. The sensor principle is laser triangulation. With the eight PDs arranged in concentric circles around the VCSEL, the influences of mirror tilt and changes in mirror reflectivity are expected to be eliminated. This sensor can measure linear displacement within an accuracy of 0.856 % F.S. at 200 µm, and 1.11 % F.S. at 500 µm. Moreover, when the tilt of the object being measured is less than 0.6°, the influence of the tilt can be ignored to some extent. In this paper, we present our method for measuring the mirror displacement and removing any influences of mirror tilt and change in mirror reflectivity.

Keywords: Displacement Sensor, Optical MEMS, Control Micro-Mirror Device

1. INTRODUCTION

Optical measuring technology achieved outstanding development due to the invention of the laser in the 1960s. Moreover, the invention of semiconductor lasers in the 1970s made it possible to commercialize optical sensors. Recently, optical sensors are in use in many industries such as automotive, robotics, medical equipment, etc. Optical sensors have many merits such as high accuracy, high functionality, and low cost. However, their cumbersome alignment and difficult miniaturization are known problems of optical sensors.

The optical displacement sensor we developed is 3.0 x 3.0 mm square and 1.3 mm thick and fabricated using MEMS technology. This sensor has a very simple structure because it requires few components, and as such, complicated alignment and assembly are not necessary when making the sensor.

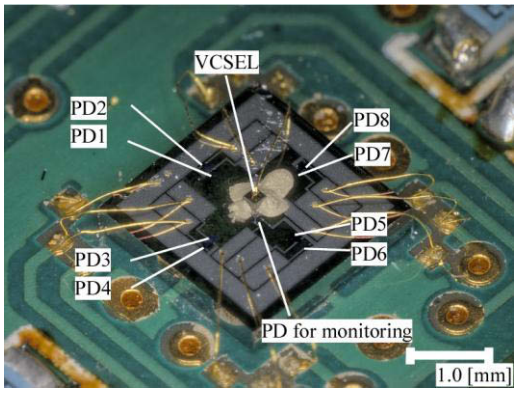

Fig. 1 Photograph of the developed sensor

For optical sensors that use laser triangulation as their measuring principle, a difficult issue occurs when the object being measured is tilted or the mirror's reflectivity is changed [1–3]. However, our sensor is expected to eliminate these influences easily due to the multiple detection area integrated on the sensor chip. We will describe our method for measuring and removing the influences of mirror tilt and changes in mirror reflectivity

2. DESIGN AND PRINCIPLE

Fig. 1 shows a photograph of the displacement sensor we have developed. The sensor size is 3.0 x 3.0 mm square and 1.3 mm thick, and it is fabricated using MEMS technology. As shown in the figure, the sensor consists of a vertical cavity surface-emitting laser (VCSEL) (SS85-5U001, Optwell Co), eight detecting photodiodes (PDs), and one monitoring PD surrounding the VCSEL. PD-1, PD-3, PD-5, PD-7 and PD-2, PD-4, PD-6, PD-8 are arranged respectively in concentric circles around the VCSEL.

The photodiodes are monolithically integrated on a silicon wafer base, and a VCSEL chip is bonded onto the base. A metal frame is then bonded onto the

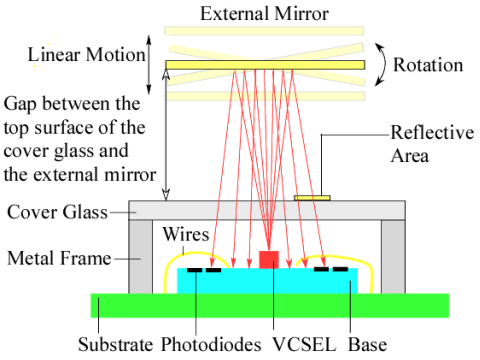

Fig. 2 Diagram of sensor principle

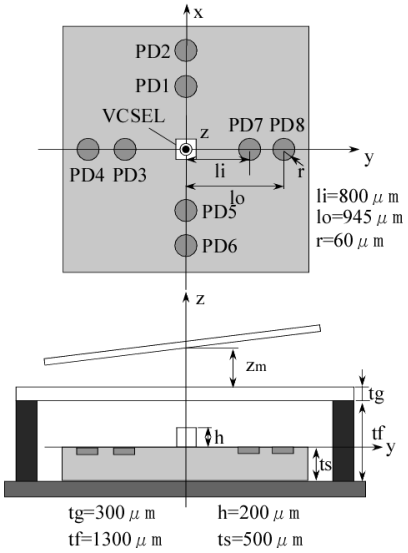

Fig. 3 Diagram of sensor structure

substrate. Onto the frame a cover glass is set with a reflective film deposited on the glass for detecting a portion of the light emitting from the VCSEL at the monitoring PD. A portion of the laser beam emitted from the central VCSEL enters the eight PDs after being reflected from external objects such as an external mirror. When the external objects are linearly moved or tilted, the diameter and the intensity of the light beam received at the photodiodes change as shown in Fig. 2. The measuring range is the region in which the signals of the detected photodiode change proportionately with the linear movement. To detect the linear distance we use the sum of the inner photodiode signals or outer photodiode signals, as shown by equation (1) or (2). P_n is the output of PD-n.

$$S_{disi} = P_1 + P_3 + P_5 + P_7 \quad (1)$$

$$S_{diso} = P_2 + P_4 + P_6 + P_8 \quad (2)$$

The structure of the four PDs located on the inner and outer concentric circles of this sensor makes it possible to avoid undesirable influences caused by minute tilting of the mirror that occurs in linear motion and changes in the reflectivity of the mirror. Fig. 3 shows our sensor structure.

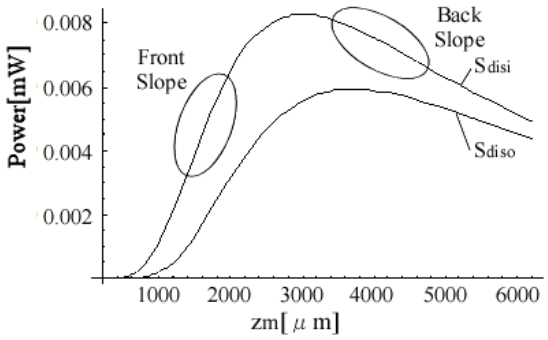

Fig. 4 Theoretical S_{disi} and S_{diso} versus z_m (x is 0° and y is 0°)

3. THEORETICAL

3.1. Linear motion

When the external mirror moves from the sensor surface at a steady speed in a direction vertical to the surface of the sensor, the signals are calculated under the assumption that the VCSEL emits a Gaussian TEM_{00} beam in the normal direction to the VCSEL substrate base using computational software (METHEMATICA5.1: WOLFRAM). The equation of the Gaussian beam profile is (3), (4).

$$I(x,y,z) = \frac{2P}{\pi\omega(z)^2}\exp[\frac{-2(x^2+y^2)}{\omega(z)^2}] \quad (3)$$

$$\omega(z) = zTan(\frac{a_w}{2}) \quad (4)$$

In these equations, P, w, z and a_w are the power of VCSEL output, beam radius, light path length, and Beam Divergence ($1/e^2$) respectively. Fig. 4 shows Sdisi and Sdiso signals when the external mirror moves linearly from the surface of the sensor (i.e., from the top surface of the cover glass) to 6000 μm away. In this figure, z_m is the gap between the top surface of the cover glass and the external mirror. In this paper, θx is the mirror tilt around the x axis, and θy is the mirror tilt around the y axis. Using this calculation, θx is 0°, andθy is also 0°. The signal has one peak for the linear motion of the external mirror and consequently a front slope and back slope are formed. The front slope and the back slope are expected to be effective for the accurate detection of minute displacements and for long-range displacements, respectively. The measurement ranges correspond to the linear region of the slopes.

3.2. Removing the influence of mirror tilt

Tilting of the external mirror influences the signals of the eight PDs. Fig. 5 shows the eight PD signals and the sum of the inner PD output and the outer PD output when the external mirror moves linearly as in the calculation in section 3.1. Then, θx is 0.6° and θy is 0°. Using these outputs, a_n, which is the bias for each output of the PDs to remove the mirror tilt influence, is calculated in the following way.

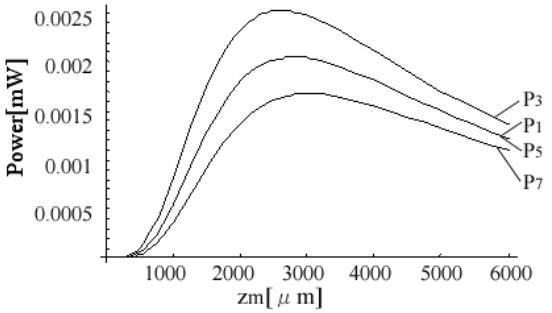

Fig. 5 Outputs of inner PDs versus z_m when θx is 0.6° and θy is 0°

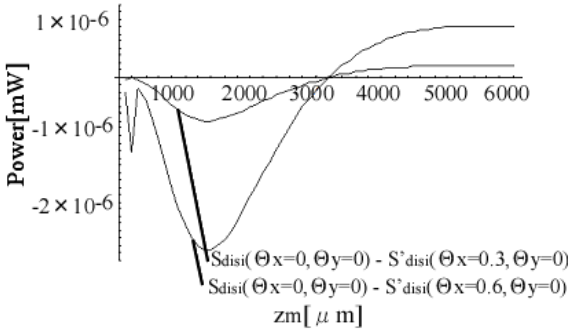

Fig. 6 Differences between S_{disi} (θx is 0° and θy is 0°) and S'_{disi} (θx is 0.3° and θy is 0°) and S'_{disi} (θx is 0.6° and θy is 0°)

The position of the center of the light spot on the sensor surface is changed because of the external mirror tilt. The center position on the sensor surface is defined as (x_c,y_c). When the external mirror is tilted, the beam profile on the sensor surface is represented by (5).

$$I'(x,x_c,y,y_c,z) = \frac{2P}{\pi(z)^2}\exp[\frac{-2\{(x-x_c)^2+(y-y_c)^2\}}{\omega(z)^2}] \quad (5)$$

As a few degrees of mirror tilt are expected, the differences in the distances from the surface of each PD to the external mirror are ignored. From (3), (4), and outputs of the eight PDs, x_c, y_c, and z are calculated. The bias for PD-n, v_n, is defined by (6).

$$v_n = \frac{I'(x_n,0,y_n,0,z)}{I'(x_n,x_c,y_n,y_c,z)} \quad (6)$$

(x_n,y_n) is the position of the center of PD-n on the sensor surface. In addition, S_{disi} and S_{diso} which removed the mirror tilt influence are defined by (7) and (8). Fig. 6 shows the differences between S_{disi} (where θx is 0° and θy is 0°) and S'_{disi} (where θx is 0.3° and θy is 0°) and S'_{disi} (where θx is 0.6° and θy is 0°). Compared with the output shown in Fig. 5, these differences are very small.

$$S'_{disi} = v_1P_1 + v_3P_3 + v_5P_5 + v_7P_7 \quad (7)$$

$$S'_{diso} = v_2P_2 + v_4P_4 + v_6P_6 + v_8P_8 \quad (8)$$

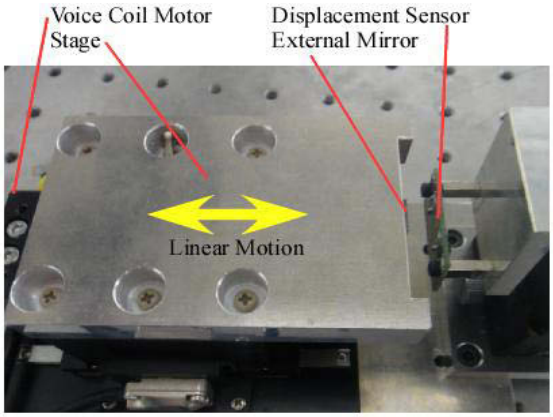

Fig. 7 Experimental system

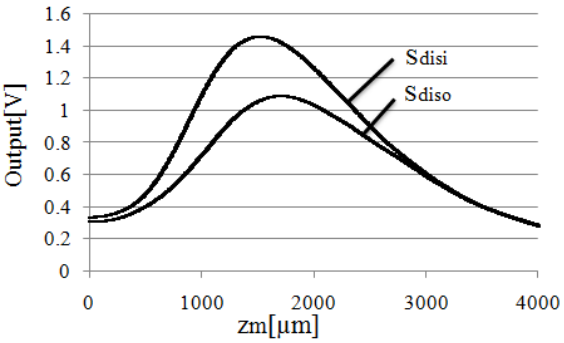

Fig. 8 Experimental S_{disi} and S_{diso} versus z_m (θx is 0° and θy is 0°)

3.3. Removing the influence of reflectivity

If we ignore any alignment error in fabrication and assembly, the signals S'_{disi} and S'_{diso} are affected by only the reflectivity of the external mirror. Therefore, only by multiplying S'_{disi} and S'_{diso} by the inverse of the reflectivity of the object being measured, it is possible to remove the influence of reflectivity. Moreover, even if the reflectivity is unknown, it can be estimated by comparing the peak values of S'_{disi}. The reflectivity is calculated by (9)

$$R = \frac{\text{Peak}_1}{\text{Peak}_2} \quad (9)$$

In this equation, Peak_n and R are the peak value of S'_{disi} when using mirror_n and the relative reflectivity of mirror1 compared with mirror2.

4. EXPERIMENTAL

4.1. Linear motion with a minute mirror tilt

Our experimental system is shown in Fig. 7. We obtained data when the external mirror moved linearly 6000 μm away from the sensor surface. Before the experiment on removing the mirror tilt influence was performed, the tilting of the external mirror was adjusted to make the outputs of the inner PDs the same as the outputs of the outer PDs. The adjusted

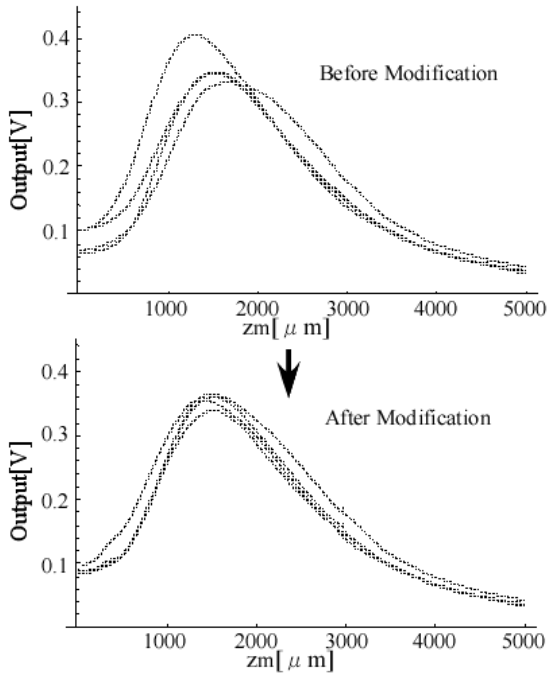

Fig. 9 Outputs of inner PDs and modified outputs of inner PDs (θx is 0.6° and θy is 0°)

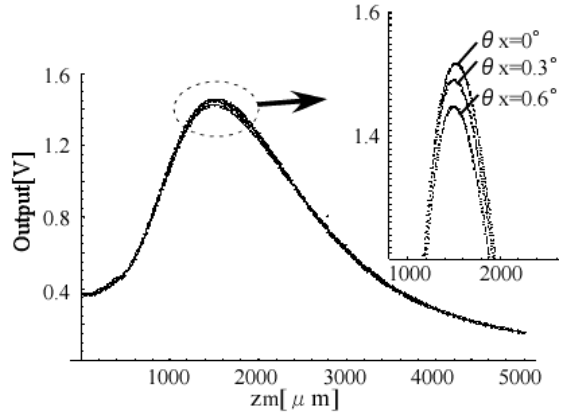

Fig. 10 S'_{disi} signal when θx is 0°, 0.3° and 0.6°.

mirror tilts around the two axes are defined as θx=0° and θy=0°. Fig. 8 shows the S_{disi} and S'_{diso} of the motion detected using our sensor when θx=0° and θy=0°. The mirror used is an Al mirror (TFAN-10C-05-10, SIGMA KOKI). These signals indicate that, at a minimum, our sensor can measure mirror displacement within an accuracy of 0.856 % F.S. at 200 µm (755 µm to 955 µm from the top surface of the cover glass) of the measurement range in the front slope portion, and 1.11 % F.S. at 500 µm (1960 µm to 2460 µm from the top surface of the cover glass) of the measurement range in the back slope portion.

4.2. Removing mirror tilt

When θx was 0°, 0.3°, 0.6°, 1°and θy was 0°, we obtained the outputs of the linear motion. The outputs were modified theoretically. Fig. 9 shows the outputs of the inner PDs and the theoretically modified linear

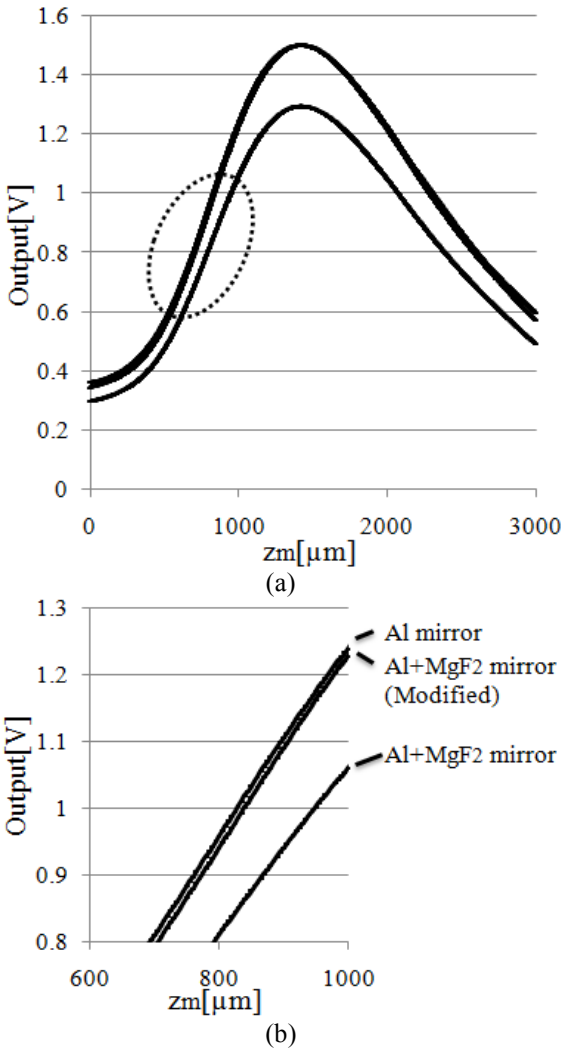

Fig. 11 (a) S'_{disi} when the external mirror is Al and Al+MgF_2, and when the influence of the reflectivity of these mirrors is removed.
(b) Detail of dotted line region

outputs of the inner PDs when θx is 0.6°. The modified outputs became nearly uniform. Fig. 10 shows the result of S'_{disi} when θx was 0°, 0.3° and 0.6°. Around the peak value, the differences between the signals when the mirror is tilted and the signal when θx is 0° is the largest. Also, the larger the mirror tilt is, the larger the differences are.

4.3. Removing the influence of reflectivity

Next, we obtained the signals of each PD when three types of mirrors were moved linearly from our sensor surface. The two types of mirrors were Al mirror (TFAN-10C-05-10, SIGMA KOKI), and Al+MgF_2 mirror (TFA-10C-05-10, SIGMA KOKI). The signals were obtained when θx was 0° and θy was 0°, and we obtained the peak values of each of the mirrors. These signals removed the influence of the mirror tilt as in the above method. The relative reflectivities of the Al+MgF_2 mirror was calculated by (6). By multiplying the inverse of this reflectivities

with the signals, we obtained the result shown in Fig. 11. In front slope, the modified signals is not same as the signal of Al mirror with a high accuracy. The possible reasons are mentioned in DISCUSSION section.

5. ANOTHER APPLICATION TO GAUGING THE DISTANCE FOR HUMAN SKIN

Optical technology is widely used in medical fields. As medical technology requires more precise and smaller sized devices, MEMS technology is being adopted for fabricating medical devices. In particular, for internal surgical procedures, it is very important to accurately gauge the distance to internal organs. With this requirement in mind, we studied distance measurements to human skin using our micro-displacement sensor.

We performed linear motion experiments using a flat scattering board and the skin of the finger tip. Since human skin is uneven and can easily be deformed, the starting state was set to be when the sensor surface just touched the skin with no force on each other. Fig. 12 shows the experiment data taken from the scattering board and the human skin of two subjects. The signal was much smaller than that from mirror experiment, which enlarged the noise influence. Also, the signal showed no front slope, but only the back slope. With the effect of the uneven surface of the skin, the signals of the skin were a little smaller and had less noise than that of the scattering board. By applying a suitable experimental modification, such as using a filter, finger stabilizer, etc., it would be possible to obtain a smooth signal such as from a scattering board. And, using the back slope of the signal, we could still calculate the distance to the skin. Furthermore, the signal did not show a large difference from person to person. Therefore, the skin characteristics and slit of the surface had few effects on the experimental results. The small individual differences indicated that distance-measuring of the skin could be achieved more easily.

6. DISCUSSION

When the mirror tilt was less than 0.6°, the influence of the tilt was removed to some extent. In fact, the beam profile of the VCSEL we used is not exactly a Gaussian TEM_{00} beam. However, the influence of the mirror tilt was removed to some extent in the way we proposed from the result of Fig. 9. To remove the influence of a larger tilt and achieve higher accuracy in this way, we need to use a VCSEL with a beam profile that is nearer to a Gaussian beam profile or find a way to calculate the beam profile of the VCSEL that approximates a Gaussian beam profile, and we also need to optimize the positions of the PDs.

The influence of reflectivity was removed to some extent, but not enough to be able to measure

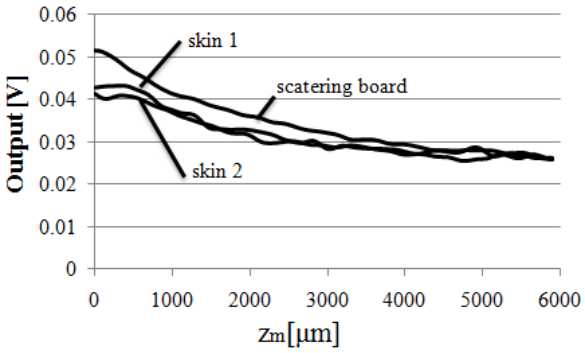

Fig. 12 S_{disi} when a scattering board and human skin are used as the object being measured.

displacement at high accuracy without relying on the material of the object being measured. There are two possible reasons. First, it is shown in Fig.11 that the refractivities are not constant values and depend on z_m. This is because the refractivity depends on the reflected angle, and the characteristics of the dependence of the reflected angle differ depending on the mirror materials. Second, from result in Fig. 10, the difference in the value of S'_{disi} is largest around the peak value of S'_{disi}. Because we used the peak value of S'_{disi} to remove the influence of reflectivity, the result is inadequate.

7. CONCLUSION

We proposed a highly accurate ultra-micro-displacement sensor with a simple structure that is easily fabricated by only bonding a VCSEL chip onto a silicon wafer with monolithically integrated PDs, a frame, and a cover glass. We have demonstrated that our sensor can measure linear displacement within an accuracy of 0.856 % F.S. at 200 μm, and 1.11 % F.S. at 500 μm. Moreover we proposed methods for removing the influence of the mirror tilt and reflectivity.

Since mirror tilt can be calculated using signals detected by our sensor, we expect the sensor to be used to control micro-mirror devices like PZT micro-mirrors, comb-drive micro-mirrors, etc. [4]. Moreover, we propose the application of our sensor for measuring displacement from human skin.

REFERENCES

[1] S V Mikhlyaev, Influence of a Tilt of Mirror Surface on the Measurement Accuracy of Laser Triangulation Rangefinder, 2006 *J. Phys.: Conf. Ser.* 48 739

[2] I. Ishikawa, R.Sawada, E.Higurashi, Integrated micro-displacement sensor that measures tilting angle and linear movement of an external mirror, Sensor and Actuators. A138 (2007) 269-275

[3] T. Ito, R. Sawada, E. Higurashi, Integrated micro-displacement sensor that uses beam divergence, J. Micromech. Microeng. 13 (2003) 942-947.

[4] T.Akase, R.SAWADA, E. Higurashi, T. Kobayashi, R. Maeda, M.Inokuchi, S. Sanada, and I. Ishikawa,

Combined Device of Optical Microdisplacement Sensor and PZT-Actuated Micromirror, IEEE/LEOS International Conference on Optical MEMS & Nanophotonics 2007, (12-16.Aug.,2007, Hualien, Taiwan),ThB5, pp.199-200

Authors: Toshihiro Takeshita, Graduate School of Systems Life Sciences, Kyushu University, 819-0395, 744, Motooka, nishi-ku, Fukuoka-city, Japan, 092-802-3241, takeshita@nano-micro.mech.kyushu-u.ac.jp. Yao Peng, Graduate School of Systems Life Sciences, Kyushu University, 819-0395, 744, Motooka, nishi-ku, Fukuoka-city, Japan, 092-802-3241, pengyao@nano-micro.mech.kyushu-u.ac.jp. Morita Nobutomo, Graduate School of Systems Life Sciences, Kyushu University, 819-0395, 744, Motooka, nishi-ku, Fukuoka-city, Japan, 092-802-3241,morita@nano-micro.mech.kyushu-u.ac.jp Hideyuki Ando, Fuzzy Logic Systems Institute, 680-41, Kawazu, Iizuka-city, Fukuoka, Japan, 0948-24-2771, ando01@hibikino.ne.jp, Eiji Higurashi, Research Center for Advanced Science and Technology Tokyo University, 153-8904, 4-6-1, Komaba, Meguro, Tokyo, Japan, 03-5452-5180, eiji@su.t.u-tokyo.ac.jp, Renshi Sawada, Department of Intelligent Machinery and Systems, Kyushu University, 819-0395, 744, Motooka, nishi-ku, Fukuoka-city, Japan, 092-802-3241, sawada@mech.kyushu-u.ac.jp,